

# The role of terrestrial vegetation in atmospheric Hg deposition: Pools and fluxes of spike and ambient Hg from the METAALICUS experiment

Jennifer A. Graydon,<sup>1</sup> Vincent L. St. Louis,<sup>1</sup> Steve E. Lindberg,<sup>2</sup> Ken A. Sandilands,<sup>3</sup> John W. M. Rudd,<sup>4</sup> Carol A. Kelly,<sup>4</sup> Reed Harris,<sup>5</sup> Michael T. Tate,<sup>6</sup> Dave P. Krabbenhoft,<sup>6</sup> Craig A. Emmerton,<sup>1</sup> Hamish Asmath,<sup>7</sup> and Murray Richardson<sup>8</sup>

Received 4 January 2011; revised 9 January 2012; accepted 22 January 2012; published 13 March 2012.

[1] As part of the Mercury Experiment to Assess Atmospheric Loading in Canada and the U.S. (METAALICUS), different stable Hg(II) isotope spikes were applied to the upland and wetland areas of a boreal catchment between 2001 and 2006 to examine retention of newly deposited Hg(II). In the present study, a Geographical Information Systems (GIS)-based approach was used to quantify canopy and ground vegetation pools of experimentally applied upland and wetland spike Hg within the METAALICUS watershed over the terrestrial loading phase of the experiment. A chemical kinetic model was also used to describe the changes in spike Hg concentrations of canopy and ground vegetation over time. An examination of the fate of spike Hg initially present on canopy vegetation using a mass balance approach indicated that the largest percentage flux from the canopy over one year post-spray was emission to the atmosphere (upland: 45%; wetland: 71%), followed by litterfall (upland: 14%; wetland: 10%) and throughfall fluxes (upland: 12%; wetland: 9%) and longer term retention of spike in the forest canopy (11% for both upland and wetland). Average half-lives ( $t_{1/2}$ ) of spike on deciduous ( $110 \pm 30$  days) and coniferous ( $180 \pm 40$  days) canopy and ground vegetation ( $890 \pm 620$  days) indicated that retention of new atmospheric Hg(II) on terrestrial (especially ground) vegetation delays downward transport of new atmospheric Hg(II) into the soil profile and runoff into lakes.

**Citation:** Graydon, J. A., et al. (2012), The role of terrestrial vegetation in atmospheric Hg deposition: Pools and fluxes of spike and ambient Hg from the METAALICUS experiment, *Global Biogeochem. Cycles*, 26, GB1022, doi:10.1029/2011GB004031.

## 1. Introduction

[2] Mercury (Hg) is a pollutant of global concern due to emissions from energy production (especially coal-fired power plants), long atmospheric residence time and long-range transport. Anthropogenic emission of Hg to the atmosphere now roughly equals natural emissions of the metal [Lindberg et al., 2007]. Even in remote regions, atmospheric deposition of Hg has increased twofold to fivefold since pre-industrial

times [Swain et al., 1992; Munthe et al., 2007]. Inorganic Hg(II) is deposited to the landscape in precipitation and dry deposition, and can be subsequently converted to methylmercury (MeHg) in anaerobic environments including wetlands [St. Louis et al., 1994], lake sediments [Gilmour et al., 1992] and hypolimnetic waters [Eckley and Hintelmann, 2006]. MeHg readily biomagnifies through aquatic food webs [Kidd et al., 1995], and the primary route of exposure for humans is consumption of contaminated fish [Hightower and Moore, 2003]. There is now strong evidence that there is a direct relationship between atmospheric deposition of Hg(II) and fish MeHg concentrations [Munthe et al., 2007; Harris et al., 2007]. Consequently, governments of individual countries are considering Hg emission reduction legislation and the United Nations Environment Program (UNEP) is preparing a global legally binding instrument on Hg (<http://www.unep.org/hazardoussubstances/Mercury/Negotiations/INC3/tabid/3469/Default.aspx>).

[3] While fish MeHg concentrations will likely decline initially in response to decreased deposition of Hg directly to lake surfaces, many lakes receive a significant portion of their annual Hg input in runoff from upland areas [Harris et al., 2007]. Large stores of Hg exist in upland vegetation

<sup>1</sup>Department of Biological Sciences, University of Alberta, Edmonton, Alberta, Canada.

<sup>2</sup>Oak Ridge National Laboratory, Oak Ridge, Tennessee, USA.

<sup>3</sup>Freshwater Institute, Fisheries and Oceans Canada, Winnipeg, Manitoba, Canada.

<sup>4</sup>R&K Research Inc., Salt Spring Island, British Columbia, Canada.

<sup>5</sup>Reed Harris Environmental Ltd., Oakville, Ontario, Canada.

<sup>6</sup>Water Resources Division, U.S. Geological Survey, Middleton, Wisconsin, USA.

<sup>7</sup>Department of Geography, University of Toronto, Mississauga, Mississauga, Ontario, Canada.

<sup>8</sup>Department of Geography and Environmental Studies, Carleton University, Ottawa, Ontario, Canada.

and especially in soils; amounts much greater than that which is deposited to landscapes annually. These historically accumulated pools of Hg can act as sources to aquatic systems that are independent of current Hg deposition, thereby dampening and delaying the effects of decreased Hg emissions on reducing fish MeHg concentrations. For example, this phenomenon was observed during a study in Gårdsjön, Sweden, where a small upland boreal catchment was covered with a roof for 10 years to remove the wet deposition of Hg [Hultberg *et al.*, 1995]. At the conclusion of the study, there was no significant difference in concentration or yield of Hg(II) in runoff from experimental and uncovered reference catchments [Munthe and Hultberg, 2004]. Export of Hg(II) was not directly affected by contemporary Hg(II) inputs because they represented only a small fraction of the soil Hg pool available for runoff.

[4] Multiple factors can influence Hg transport and retention within watersheds including the size and topography of the watershed, the ratio of watershed to lake area, land use and land cover [Munthe *et al.*, 2007]. For example, the presence of forest canopies can dramatically influence Hg deposition to, and movement through, the landscape. Foliage accumulates atmospheric Hg(0) via stomata and deposition to leaf cuticles [Converse *et al.*, 2010] and foliar surfaces adsorb both particulate Hg (PHg) and reactive gaseous Hg (RGM) from the atmosphere. Deposition of Hg beneath forest canopies in throughfall and litterfall therefore far exceeds deposition of Hg in adjacent open areas [Rea *et al.*, 1996; Grigal *et al.*, 2000; Lee *et al.*, 2000; St. Louis *et al.*, 2001; Graydon *et al.*, 2008]. As the first watershed compartment that Hg(II) in precipitation contacts in forested areas, trees (and below them ground vegetation species) have the capacity to intercept and retain Hg over unknown periods of time, possibly until senescence and decomposition of litterfall [Hall and St. Louis, 2004; Graydon *et al.*, 2006].

[5] While previous Hg mass balance studies of watersheds have determined that uplands are sinks for atmospheric Hg [Johansson *et al.*, 1991; Munthe and Hultberg, 2004], the dynamics of these systems cannot be determined by this approach because it is impossible analytically to distinguish new Hg from older, historically deposited Hg once it is deposited to the landscape. These studies provided little information about the mobility of Hg(II) from individual deposition events, or the residence times of newly deposited Hg(II) in different watershed compartments. These questions have been investigated most recently by experiments using stable Hg isotopes, which have allowed researchers to trace the biogeochemical movement of newly deposited Hg within ecosystems [e.g., Hintelmann *et al.*, 2002; Graydon *et al.*, 2006; Harris *et al.*, 2007]. The Mercury Experiment to Assess Atmospheric Loading in Canada and the U.S. (METAALICUS) conducted at the Experimental Lakes Area (ELA) has combined a whole-ecosystem experimental approach with the use of enriched stable Hg isotope “spikes” to investigate the magnitude and timing of the response of fish MeHg concentrations to changes in atmospheric Hg(II) loadings. In addition to applying spike Hg to the lake itself, the upland and wetland portions of the watershed were also loaded to examine residence times within the forest canopy, ground vegetation and soils, and fluxes of spike Hg among these watershed compartments [Sandilands *et al.*, 2005]. Kinetic data describing the movement of Hg

within a natural ecosystem produced by the METAALICUS experiment is extremely rare in the literature and represents critical information for 1) modelers working on global Hg cycling mass balance models and 2) international policy makers evaluating the effectiveness of proposed Hg emissions reductions worldwide toward lowering fish MeHg concentrations.

[6] The objectives of this study were to: 1) describe the retention of new, experimentally wet-deposited atmospheric Hg within canopy and ground vegetation of a boreal upland and wetland over 6 years of experimental loading of isotopic Hg(II) and 2) generate kinetic data on the movement of new atmospheric Hg following wet deposition to canopy vegetation by examining re-emission, throughfall and litterfall fluxes from this compartment.

## 2. Methods

### 2.1. Site Description

[7] METAALICUS was conducted within the Lake 658 lake and watershed at the ELA. The ELA is located on the Precambrian shield in Northwestern Ontario, Canada and includes 58 experimental lakes and watersheds set aside for whole-ecosystem experimentation [Stokstad, 2008]. Lake 658 is 8 ha in surface area, surrounded by a 43 ha watershed (Figure 1a). The lake is located at 49° 43.95' N latitude and 93° 44.2' W longitude and is comprised of west and east basins partly separated by a bedrock peninsula extending from the North shoreline. The outflow of Lake 658 drains into large (24.5 km<sup>2</sup>), oligotrophic Winnange Lake.

[8] Four distinct forest types occur within the Lake 658 watershed (Figure 1b): 1) a 6 ha area in the northwest portion of the watershed was clear-cut logged in 1978 and now supports a deciduous forest of red maple (*Acer rubrum*), white birch (*Betula papyrifera*) and trembling aspen (*Populus tremuloides*; max. canopy height = 9 ± 4 m); 2) in 1983, a forest fire burned most of the southern portion of the watershed and a section of the northern shore and this 21 ha burned area now contains a dense canopy of young, fire-regenerated jack pine (*Pinus banksiana*; max. canopy height = 7 ± 3 m; aerial photos from 1982 and 1991 were used to delineate logged and burned areas, respectively); 3) the portion of the upland that was not burned or logged (14 ha) is dominated by mature black spruce (*Picea mariana*) and balsam fir (*Abies balsamea*) forest (max. canopy height = 14 ± 5 m); and 4) a 2 ha wetland that extends back from the west basin is comprised of black spruce, jack pine and alder shrubs (*Alnus sp.*; max. canopy height = 7 ± 3 m).

### 2.2. Spike Hg Applications

[9] Between 2001 and 2006, upland and wetland portions of the Lake 658 watershed were sprayed annually with enriched <sup>200</sup>Hg(II) (80%) and <sup>198</sup>Hg(II) (91%) spike solutions, respectively. Upland and wetland spike solutions were mixed into water from nearby large oligotrophic Eagle Lake (Winnange Lake flows into Eagle Lake) immediately prior to deposition. Upland and wetland areas were sprayed using a Cessna 188 AG truck crop-duster aircraft. For the purpose of spike application, the large Lake 658 upland (41 ha) had to be divided into several smaller areas that were compatible with the spike solution holding capacity of the aircraft (details in the work by Sandilands *et al.* [2008]).

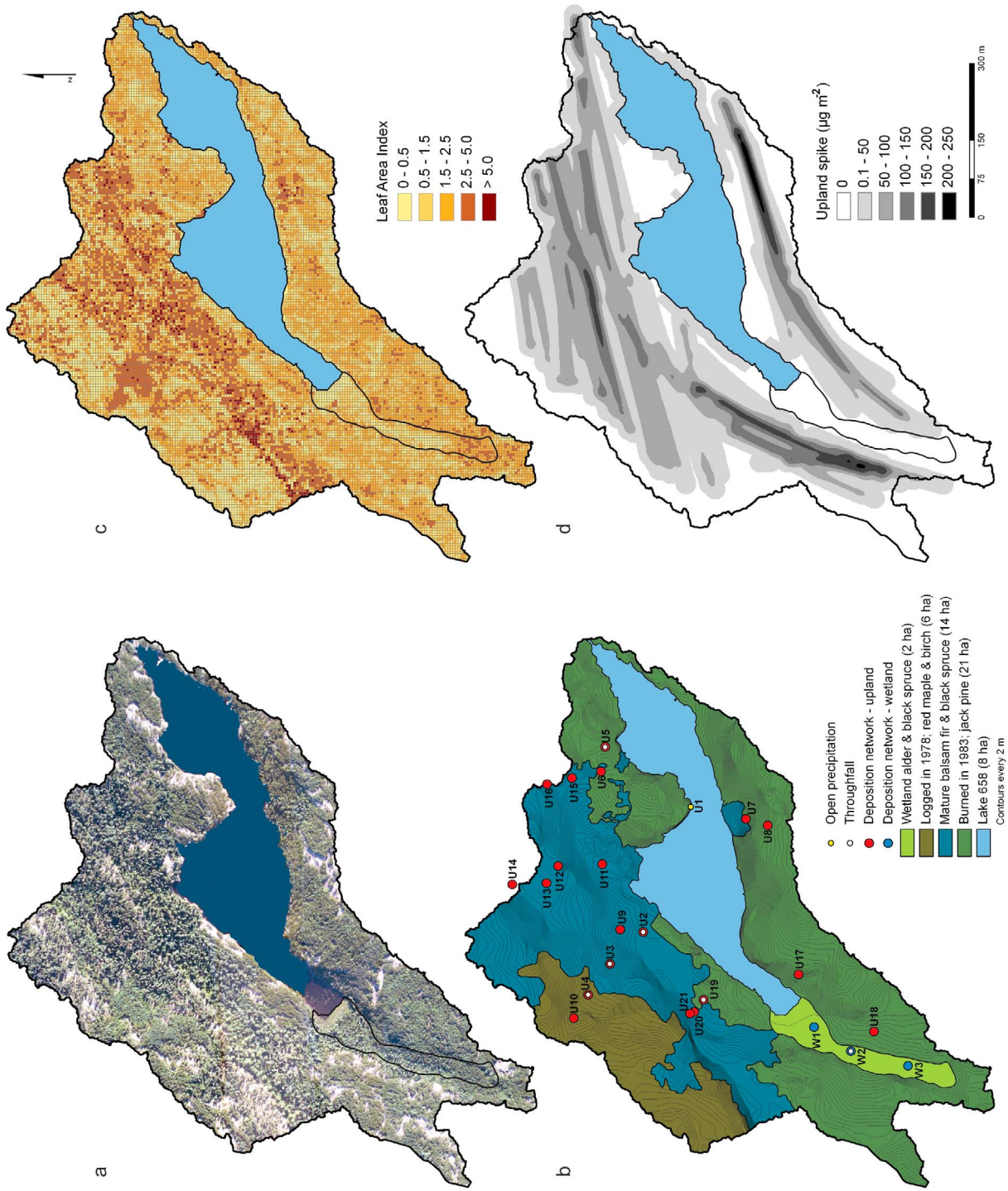


**Figure 1.** (a) Aerial photograph of Lake 658 and watershed, (b) forest type map and locations of sampling sites, (c) leaf area index map, and (d) 2006 upland spike spray map.

**Table 1.** Average Application Rates of Upland and Wetland Spike to the METAALICUS Watershed Between 2001 and 2006 Including Both Annual Aerial and Shoreline Applications<sup>a</sup>

Year	Average Upland Spike Application Rate ( $\mu\text{g m}^{-2}$ )	Average Wetland Spike Application Rate ( $\mu\text{g m}^{-2}$ )
2001	13.28	18.63
2002	20.61	2.73
2003	22.65	41.34
2004	15.10	5.10
2005	1.12	1.24
2006	38.31	37.96

<sup>a</sup>Modified from *Sandilands et al.* [2008].

Upland and wetland spike applications occurred immediately before or during natural rain events, and had to be performed under low-wind conditions to ensure pilot and aircraft safety. Because of these strict environmental requirements and the size of the watershed, weather conditions rarely permitted the application of spike to all upland and wetland areas on the same day. To avoid accidental overspray of terrestrial spike Hg from the aircraft into the lake, spraying of upland and wetland shorelines was completed from a barge with a firehose, using water from Winnange Lake and Hg spike introduced into the nozzle flow. The lake itself was spiked with enriched  $^{202}\text{Hg}(\text{II})$  (90%) in the propeller wash of an electric boat motor as the boat drove around the lake after sunset. The overall target spike application rate to all areas was  $22 \mu\text{g m}^{-2} \text{yr}^{-1}$ , approximately 6 times the long-term (1990–2006) average deposition of Hg in open area precipitation to the area ( $3.6 \mu\text{g m}^{-2} \text{yr}^{-1}$ ) [Graydon *et al.*, 2008]. Actual annual upland and wetland spike application rates sometimes differed substantially from this target due to inclement weather and pilot availability (Table 1, modified after *Sandilands et al.* [2008]).

[10] Maps of each terrestrial spray event (i.e., each spike application to individual upland and wetland subdivisions) were generated using the aircraft's global positioning system (GPS) flight track and the spike application rate during each flight. Recording of GPS coordinates by the aircraft occurred at a constant rate during spraying and the spike application rate was also constant, allowing the mass of Hg sprayed at each GPS point to be calculated [Sandilands *et al.*, 2008]. The density of GPS points within a radius of 20 m was calculated using the kernel function in Spatial Analyst [20 m was the distance the spray was expected to drift out from the flight path of the aircraft under the low wind conditions that were required for spraying to occur (A. Robinson, personal communication, 2001). This calculated density was then multiplied by the amount of Hg sprayed at each GPS point, to give a spatial map of the amount of spike Hg applied throughout the watershed. Overlapping flight paths were taken into account, and individual spray events to different upland subdivisions (including shoreline spray events) were summed together to calculate annual spike Hg application maps (hereafter referred to as "spray maps") for each year between 2001 and 2006 (e.g., Figure 1d shows the 2006 upland spray map and Figures S1 and S2 in the auxiliary material show all spray maps for upland and wetland areas, respectively, between 2001 and 2006).<sup>1</sup>

<sup>1</sup>Auxiliary materials are available in the HTML. doi:10.1029/2011GB004031.

### 2.3. Sample Collection

[11] Pools (forest canopy and ground vegetation) and fluxes (open precipitation, throughfall and litterfall) of spike and ambient Hg within the Lake 658 watershed were calculated using concentrations from representative samples collected at sites within each forest type. A network of sampling sites along seven transects was established within the watershed with eleven sites sampled initially in 2001 (U1–U8 and W1–W3, Figure 1b). Thereafter, 24 sites were sampled. Locations of sampling sites were mapped within  $< 1$  m using a Trimble Geo XT handheld field computer with a built-in submeter GPS receiver.

[12] Canopy vegetation (terminal boughs  $\sim 45$  cm in length including branches, new and old foliage) was clipped from trees at a height of 3–4 m above ground using a pole pruner, and caught using gloved hands. At densely treed, mature fir/spruce sites, it is possible that samples may have contained less spike Hg than would have been found in foliage at the top of those trees. However, at other sites, trees were more spread out and the foliage sampled at 3–4 m would have received spray directly from the plane and been completely consistent with spike concentrations near the tree tops. At yet other sites, trees located on the edges of clearings were sampled and these would also have received spray directly from the aircraft. Sampling sites included enough different sites (i.e., along the continuum between sparse to densely treed and from the four different forest types), that samples were as close to representative of the overall Lake 658 forest canopy as possible. Ground vegetation was collected within a  $225 \text{ cm}^2$  quadrat at each site. Shrubs were clipped using hand pruners and mosses and lichens were peeled from soils using gloved hands. Fresh litter within the ground vegetation layer was included in the samples. Canopy and ground vegetation samples were collected within one week prior to aerial spray applications to determine pre-spray spike and ambient Hg concentrations and then again within a few days after the spray events to determine the amount of spike present due to the spray in question. Samples were also collected one to six additional times each field season. All samples were stored frozen in Ziploc bags until they were processed and analyzed.

[13] Open area precipitation, throughfall and litterfall samples were collected and processed as described by Graydon *et al.* [2008]. One automated precipitation collector was located on the peninsula to collect open area precipitation and between 3 (2001–2004) and 6 (2005–2006) automated throughfall collectors in total were deployed throughout the watershed to collect throughfall during the non-winter season (i.e., early May to late October; Figure 1b). Two litterfall collectors were deployed at each deposition network site in the watershed and sampled in the late fall and early spring each year to create composite annual litterfall samples. The bulk of the litterfall mass flux occurs in the fall and is included in the fall sample collection. Throughfall and litterfall collectors were emptied and covered with plastic during aerial spraying to prevent excessive contamination of the collectors by the highly concentrated spike.

### 2.4. Sample Analysis

[14] Canopy, ground vegetation and litterfall samples were freeze-dried, weighed and homogenized using stainless steel coffee grinders cleaned with Milli-Q water and paper towels. All samples collected in the METAALICUS watershed

between 2001 and 2006 were analyzed using inductively coupled plasma mass spectrometry (ICP-MS) [Hintelmann *et al.*, 1995; Hintelmann and Evans, 1997]. Because ICP-MS quantifies concentrations of individual Hg isotopes, it was possible to distinguish concentrations of ambient Hg from the experimentally loaded enriched isotopic Hg spikes. To calculate concentrations of ambient Hg, an isotope that was not experimentally applied to the watershed ( $^{199}\text{Hg}$ ) was used as an ambient Hg surrogate. It should be noted that while spike solutions were greatly enriched in a given Hg isotope, they still contained minor amounts of other Hg isotopes that needed to be accounted for. Therefore, fluxes and concentrations of the enriched Hg spikes reported here represent all experimentally applied Hg(II).

[15] Open area precipitation and throughfall samples collected in 2001–2004 were analyzed at the Trent University Worsfold Water Quality Center (Peterborough, ON). Samples were continuously mixed in-line with  $\text{SnCl}_2$  using peristaltic pumps, and the reduced gaseous Hg(0) formed was separated in a custom-made gas/liquid separator and swept into the plasma of a Finnigan Element 2 ICP-MS [Hintelmann and Ogrinc, 2003]. Open area precipitation and throughfall samples collected between 2005 and 2006 were analyzed at the University of Alberta Biogeochemical Analytical Service Laboratory (BASL, Edmonton, AB). In this laboratory, reduction of Hg and gas/liquid separation was accomplished using an automated Tekran 2600 total Hg analyzer interfaced with a PerkinElmer Elan DRC-e ICP-MS for detection. Limits of detection (LODs) for ambient THg analyses were between 0.01 and 0.03  $\text{ng L}^{-1}$  for wet deposition samples. The LOD for the experimentally applied Hg isotopes varied with the precision of the isotope ratio measurement. Therefore, using the techniques described above, to detect an applied isotope with certainty, it had to be present at a concentration of at least 0.3–2.0% of the ambient Hg concentration of the sample.

[16] Canopy foliage, ground vegetation and litterfall samples were analyzed at the BASL. Sub-samples of ground plant tissues (250 mg) were digested in 60 mL Teflon bombs using 7 mL of 7:3 (vol/vol)  $\text{HNO}_3/\text{H}_2\text{SO}_4$ . Bombs were heated in a vented oven for two hours at 125°C. Samples were allowed to cool and 19 mL of Milli-Q water and 1 mL of BrCl were added. Bombs were closed and heated overnight at 60°C. A 0.5 mL subsample of the digest was diluted with Milli-Q water and hydroxylamine hydrochloride (0.04%, for neutralization) to a final volume of 50 mL. Sample reduction, delivery and detection were accomplished using an automated Tekran 2600 total mercury analyzer interfaced with a PerkinElmer Elan DRC-e ICP-MS. Spike recoveries were always > 90% and NIST pine needles 1575a was used as a standard reference material. The limit of detection (LOD) for ambient THg in plant tissue samples was 0.4  $\text{ng g}^{-1}$ . LODs for the experimentally applied Hg isotopes ranged from 0.2 to 1  $\text{ng g}^{-1}$ . All analytical laboratories successfully participated in inter-laboratory comparisons over the course of this study.

## 2.5. Modeling of Forest Canopy and Ground Vegetation Spike and Ambient Hg Pools

### 2.5.1. Watershed Characterization

[17] The boundaries of the watershed, wetland and lake were determined from a 1-m resolution bare-earth digital

elevation model (DEM) derived from an airborne Light Detection and Ranging (LiDAR) survey that was conducted in July, 2005. The wetland and lake boundaries were manually interpreted and digitized from the DEM, whereas the watershed boundary was extracted using standard digital terrain analysis techniques. Leaf Area Index (LAI) across the watershed was also modeled using the classified vegetation returns from the same LiDAR survey (Figure 1c) [Asmath, 2005]. The modeled LAI was ground-truthed using hemispherical photographs taken at each sampling site and at additional sites in the watershed [Leblanc *et al.*, 2005]. The relationship between measured and modeled LAI ( $\text{LAI}_{\text{modeled}} = 0.87 * \text{LAI}_{\text{measured}} + 0.28$ ) was highly significant ( $R^2 = 0.87$ ,  $p < 0.001$ ). The LAI map had a grid size resolution of 25  $\text{m}^2$  (0.0025 ha), as did all original input rasters (i.e., spray maps and the LAI map) and all rasters produced in the process of modeling the Hg pools and fluxes. Spatial calculations on maps were performed using the GIS software ArcMap 9.2 and raster calculator in Spatial Analyst (Environmental Systems Research Institute, ArcGIS 10 software, 2011).

### 2.5.2. Biomass

[18] To calculate the pool of spike and ambient Hg within the forest canopy, we required an estimate of canopy biomass. Canopy biomass was calculated from the LAI map (Figure 1c) and formulae relating LAI to branch plus foliar biomass in aspen, black spruce, old jack pine and young jack pine forests at eight sites in two study areas in Manitoba and Saskatchewan boreal forests [Gower *et al.*, 1997]. Biomass measurements in  $\text{kg carbon ha}^{-1}$  from Gower *et al.* [1997] were first converted to biomass estimates (in  $\text{kg ha}^{-1}$ ) by assuming that branches and foliage were 50% and 45% carbon, respectively. Average LAI was regressed against corresponding aboveground biomass in branches and foliage at sites from that study, resulting in the following relationships: black spruce: biomass ( $\text{kg ha}^{-1}$ ) =  $4421 * \text{LAI}$  ( $\text{ha ha}^{-1}$ ); jack pine: biomass ( $\text{kg ha}^{-1}$ ) =  $3793 * \text{LAI}$  ( $\text{ha ha}^{-1}$ ); aspen: biomass ( $\text{kg ha}^{-1}$ ) =  $6038 * \text{LAI}$  ( $\text{ha ha}^{-1}$ ). Formulae for black spruce, aspen and jack pine were applied to mature (spruce and fir), logged (deciduous) and burned jack pine/wetland areas, respectively, using the L658 watershed forest-types map (Figure 1b). Using these equations, aboveground biomass in branches plus new foliage and old foliage ( $\text{kg ha}^{-1}$ ; hereafter referred to as the “canopy biomass map”) was estimated from LAI values throughout the METAALICUS watershed.

[19] For ground vegetation, dry biomass of samples collected within sampling quadrats was measured and average areal biomass for sites within each of the 4 forest types within the watershed was calculated for each year of the experiment (2001–2006).

### 2.5.3. Hg Concentration and Pool Mapping

[20] The spray maps (described above in section 2.2) were used to determine the spike load delivered to individual sampling sites each year. The spike load delivered by the aircraft was regressed against the spike concentration measured in the canopy (which was first corrected for any spike that remained from the previous application event). As described in section 2.3, each tree was sampled a few days before a given year’s spike was applied and then again within a few days after the spike was applied. The pre-spray foliar

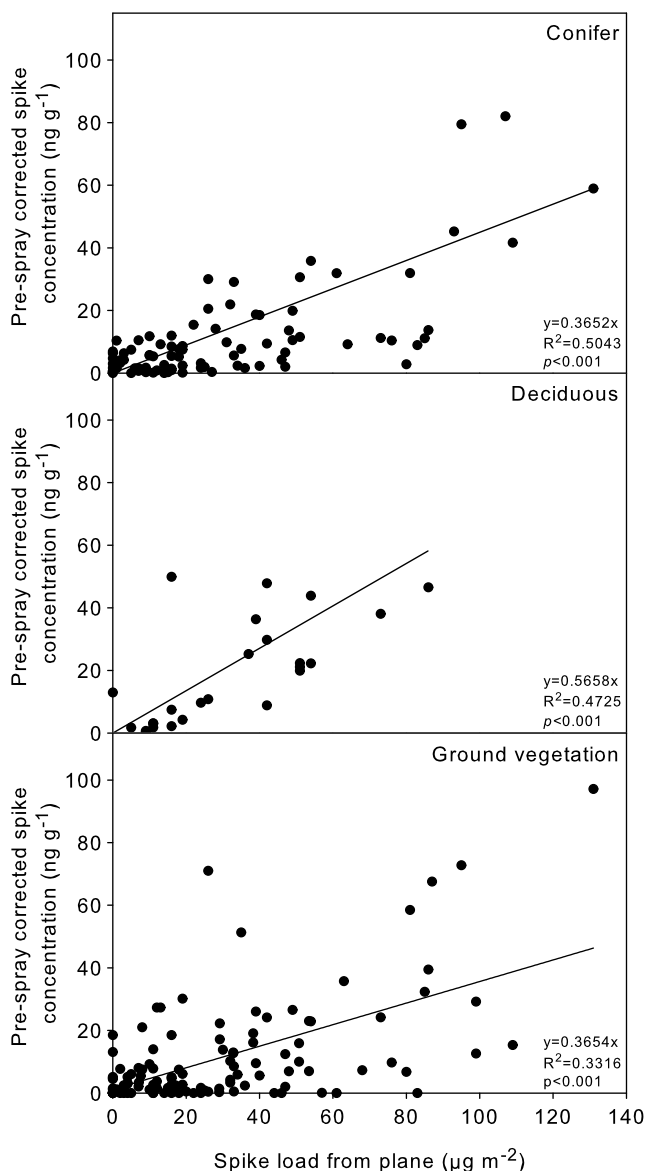


**Figure 2.** Current year spike Hg load from plane regressed against current year spike Hg concentration (i.e., after correction for any spike remaining from previous year application) of (top) conifer and (middle) deciduous canopy foliage and (bottom) ground vegetation.

spike concentration (typically small) was subtracted from the post-spray concentration to generate an estimate of the spike concentration due solely to the spray in question. In a very small number of cases (4 out of 113), the lack of a “direct hit” of spray from the plane combined with heterogeneity associated with destructive sampling and having to sample adjacent different branches resulted in negative corrected spike concentrations. It is impossible that the act of applying the spike resulted in spike being removed from tree foliage, so in these cases, post-spray spike concentration was designated as 0 and included in all further calculations. The regression relationships produced as above (Figure 2) were applied to each annual spray map to generate a map of canopy spike concentration due solely to the spray in

question. Coniferous and deciduous areas were modeled separately because of the marginally statistically significantly different slopes of the regressions for coniferous and deciduous trees (Figure 2). Using ArcGIS Desktop software, raster GIS map algebra was used to determine the total spike pools throughout the watershed. For each annual spray event, the total mass of Hg spike was determined by multiplying the canopy biomass raster by the corresponding canopy spike Hg concentration raster for both the upland and wetland portions of the watershed, resulting in a final raster map quantifying the canopy spike pool throughout the watershed ( $\mu\text{g m}^{-2}$ ). In contrast, the distribution of ambient Hg within the forest canopy was reflective of forest types, not the experimental spike loading. Therefore, for each year, the average concentration of ambient Hg measured within each forest type over all samplings was multiplied by the canopy biomass raster to generate a raster map quantifying the canopy ambient Hg pool throughout the watershed ( $\mu\text{g m}^{-2}$ ).

[21] Annual ground vegetation spike concentration maps were calculated similarly to the canopy spike concentration maps using a regression between the load of spike from the plane and the pre-spray corrected concentration of spike in ground vegetation (Figure 2). However, average areal biomass of ground vegetation within each of the four forest types was used in the calculation of the ground vegetation spike pool instead of LAI/biomass relationships. For the pool of ambient Hg in ground vegetation, the annual average ambient Hg concentration was simply multiplied by the average annual biomass.

[22] To describe the decline in upland and wetland spike Hg concentration of canopy and ground vegetation over time, a chemical kinetic model was used. To standardize the extremely variable post-spray spike concentrations of canopy foliage at different sites, the highest spike concentration observed within the first 10 days post-spray was set to 100% (in the vast majority of cases, the highest spike concentration corresponded to the first sample collected) and concentrations of subsequent samples were expressed as a % of the initial (Figure 3). In many cases, concentrations of spike in ground vegetation samples were not highest initially after the spray, so the initial sample spike concentration was always set to represent 100% (Figure 4). The natural logarithms (Ln) of the % of initial concentration data were calculated and the overall process was best described by first order reaction kinetics:

$$\text{Ln}(\% \text{ of initial [spike Hg]})_t = \text{Ln}(\% \text{ of initial [spike Hg]})_0 - kt \quad (1)$$

where  $(\% \text{ of initial [spike Hg]})_t$  and  $(\% \text{ of initial [spike Hg]})_0$  are the % of initial spike Hg concentrations at time  $t$  and 0, respectively, and  $k$  is the first-order rate constant. Half-lives of spike Hg(II) on canopy vegetation (deciduous and coniferous) and ground vegetation were calculated as follows:

$$t_{1/2} = \text{Ln}(2)/k \quad (2)$$

Decline curves for deciduous and coniferous canopies and ground vegetation were used to determine the proportion of the initial spike concentration remaining in the canopy and ground vegetation immediately prior to the next year’s spray event. These proportions were multiplied by the total post-

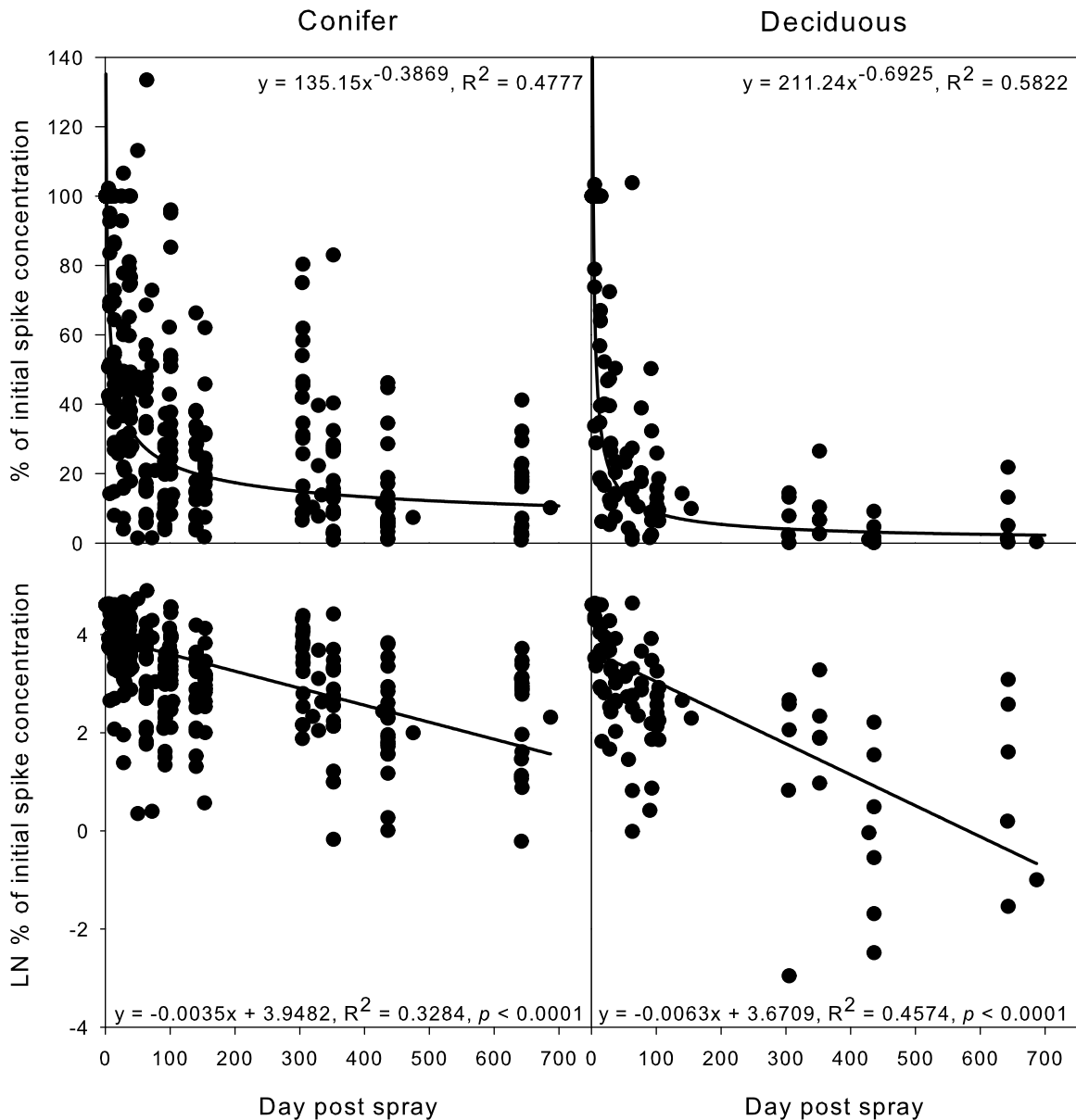


**Figure 3.** (top) Measured spike Hg concentrations of coniferous and deciduous canopy foliage expressed as the percentage of initial post-spray spike concentration (100%) and the best (power) fit line. If a canopy sample collected within the first 10 days post spray other than the first showed the highest concentration, the former was selected to represent 100%. (bottom) Ln of the percentage of initial post-spray spike Hg concentration over time and the best (linear) fit line where the slope is equal to the spike concentration decline rate constant ( $k$ ).

spray spike pool for the previous year to generate an estimate of the pre-spray upland and wetland canopy and ground vegetation pools.

#### 2.5.4. Error

[23] Relative error was propagated through the spike and ambient Hg pool calculations using the unexplained variance in all regression equations used (i.e., measured versus modeled LAI, biomass versus LAI and spike load from plane versus spike concentration regressions for canopy and ground vegetation) and relative error in ambient concentrations of canopy and ground vegetation (S.D./mean).

#### 2.6. Fate of Spike Hg in the Forest Canopy

[24] To determine the fate of the spike Hg present in the canopy immediately following each application, we quantified fluxes of spike Hg in throughfall, litterfall and re-emission to the atmosphere. Annual ambient Hg fluxes in open area precipitation, throughfall and litterfall and annual spike Hg fluxes in litterfall were calculated as by Graydon *et al.* [2008]. Estimation of spike throughfall flux was limited to the time immediately after the spray until late October when the collectors were shut down for the winter. Where throughfall snowpack samples were available, a winter (maximum

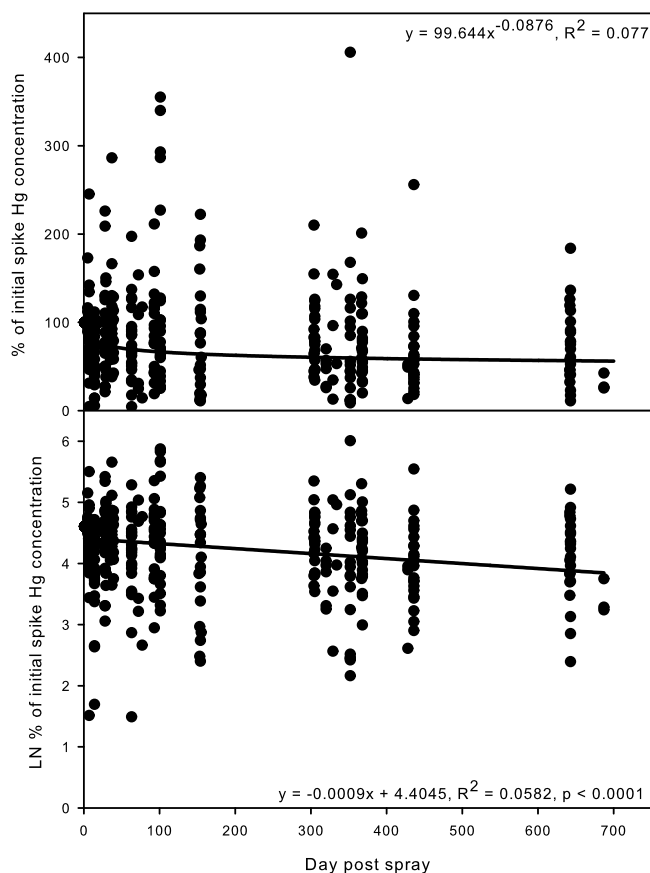


**Figure 4.** (top) Spike Hg concentrations of ground vegetation expressed as the percentage of initial post-spray spike concentration (100%) and the best (power) fit line. (bottom) Ln of the percentage of initial post-spray spike Hg concentration over time and the best (linear) fit line where the slope is equal to the spike concentration decline rate constant ( $k$ ).

snowpack; mid-March) loading of spike was also included in the annual throughfall spike flux.

[25] A dynamic flux chamber was used to quantify re-emission of spike Hg(II) as Hg(0) from canopy foliage [Graydon *et al.*, 2006]. After spike applications in 2003, re-emission of spike Hg(0) was measured from two black spruce trees and a jack pine tree in the upland forest, and from an alder shrub in the wetland. Flux measurements were performed the first day post-spray, repeated several times between 2 and 10 days post-spray, and then approximately monthly thereafter until the end of August. In all cases, flux measurements lasted 1 h and gold traps were analyzed for spike Hg(0) by ICP-MS. For consistency, all flux measurements from a given tree were performed using the same branch on every occasion. This branch was collected following the final flux measurements for determination of freeze-dried weight and leaf area. Adjacent branches were collected every time a flux measurement was performed, and at some additional times throughout the summer. Since foliar sampling and analysis was destructive, it was impossible to monitor the spike concentrations of individual leaves over the course of the experiment. Power or log curves were fit to the spike Hg(0) flux data and the total amount of spike

emitted over the next 365 days was calculated assuming that the spike Hg(0) would be emitted from foliage at the estimated rate for an average of 7 h d<sup>-1</sup>. Total spike Hg(0) emitted (ng m<sup>-2</sup>) was multiplied by LAI at the same site to express the total flux of spike per unit area. For all four trees, the initial canopy spike Hg concentration (ng g<sup>-1</sup>) was regressed against the total  $\mu\text{g m}^{-2}$  of spike Hg(0) evaded. This relationship was then applied to the post-spray canopy spike concentration maps to generate maps of spike Hg(0) evaded on an areal basis ( $\mu\text{g m}^{-2}$ ).

### 3. Results and Discussion

#### 3.1. Ambient Hg Pools and Fluxes

##### 3.1.1. Canopy

[26] Ambient Hg concentrations in tree foliage observed in this study (Figure S3) are near the low end of the range reported for canopy foliage in uncontaminated areas (10–300 ng Hg g<sup>-1</sup>) [Moore *et al.*, 1995]. Hg concentrations in leaves of trees (black spruce, jack pine, white birch and tamarack [*Larix laricina*]) and shrubs (leatherleaf [*Chamaedaphne calyculata*], labrador tea [*Ledum groenlandicum*], and speckled alder [*A. rugosa*]) collected previously at the ELA ranged from 5–23 ng g<sup>-1</sup> [Moore *et al.*, 1995; Heyes *et al.*, 1998]. The low concentrations of Hg in foliage at the ELA are consistent with the fact that this area is remote and far from any point-source contamination.

[27] Other studies have demonstrated that the ambient Hg content of leaves/needles of many tree species increases over the course of the growing season [Bombosch, 1983; Wyttenbach and Tobler, 1988; Barghigiani *et al.*, 1991; Rasmussen *et al.*, 1991; Rasmussen, 1995; Fleck *et al.*, 1999]. While ambient Hg concentrations of most deciduous species increased significantly over time in the present study, this was not the case for conifers (Figure S3), likely because samples from conifers integrated foliage from both the current and previous growing seasons. The annual ambient Hg concentrations used to model the canopy pools were determined from *all* samples collected in each area throughout the growing season of that year, thereby averaging out the low concentrations in the spring and the higher concentrations in the fall for the deciduous areas.

[28] The upland canopy ambient Hg pool (Figure 5) ranged from a low of  $8.41 \pm 3.37 \mu\text{g m}^{-2}$  in 2001, perhaps due to the lower number of trees/sites sampled that first year, to a high of  $14.3 \pm 7.78 \mu\text{g m}^{-2}$  in 2006, though pools in different years were not different within error. The wetland canopy ambient Hg pool was more constant over time than the upland, ranging only from  $4.96 \pm 2.03 \mu\text{g m}^{-2}$  in 2004 to  $5.87 \pm 2.35 \mu\text{g m}^{-2}$  in 2006. The lower areal pool of ambient Hg in the wetland is likely due to the sparser canopy in the wetland compared to the upland. Areal ambient Hg canopy pools presented here are comparable but generally lower than previously published values for this same watershed in the fall of 2003, calculated without the benefit of spatial biomass data and GIS (upland:  $17.3 \pm 23.0 \mu\text{g m}^{-2}$ , wetland:  $9.9 \pm 1.1 \mu\text{g m}^{-2}$  [Harris *et al.*, 2007]).

[29] Average annual Hg loading in open area wet deposition ( $\pm$ S.D.) to the Lake 658 watershed over the course of this study was  $3.1 \pm 2.0 \mu\text{g m}^{-2}$  [Graydon *et al.*, 2008]. Annual average Hg loadings in throughfall beneath mature spruce/fir ( $12.0 \pm 4.1 \mu\text{g m}^{-2}$ , 4.0 times open deposition),

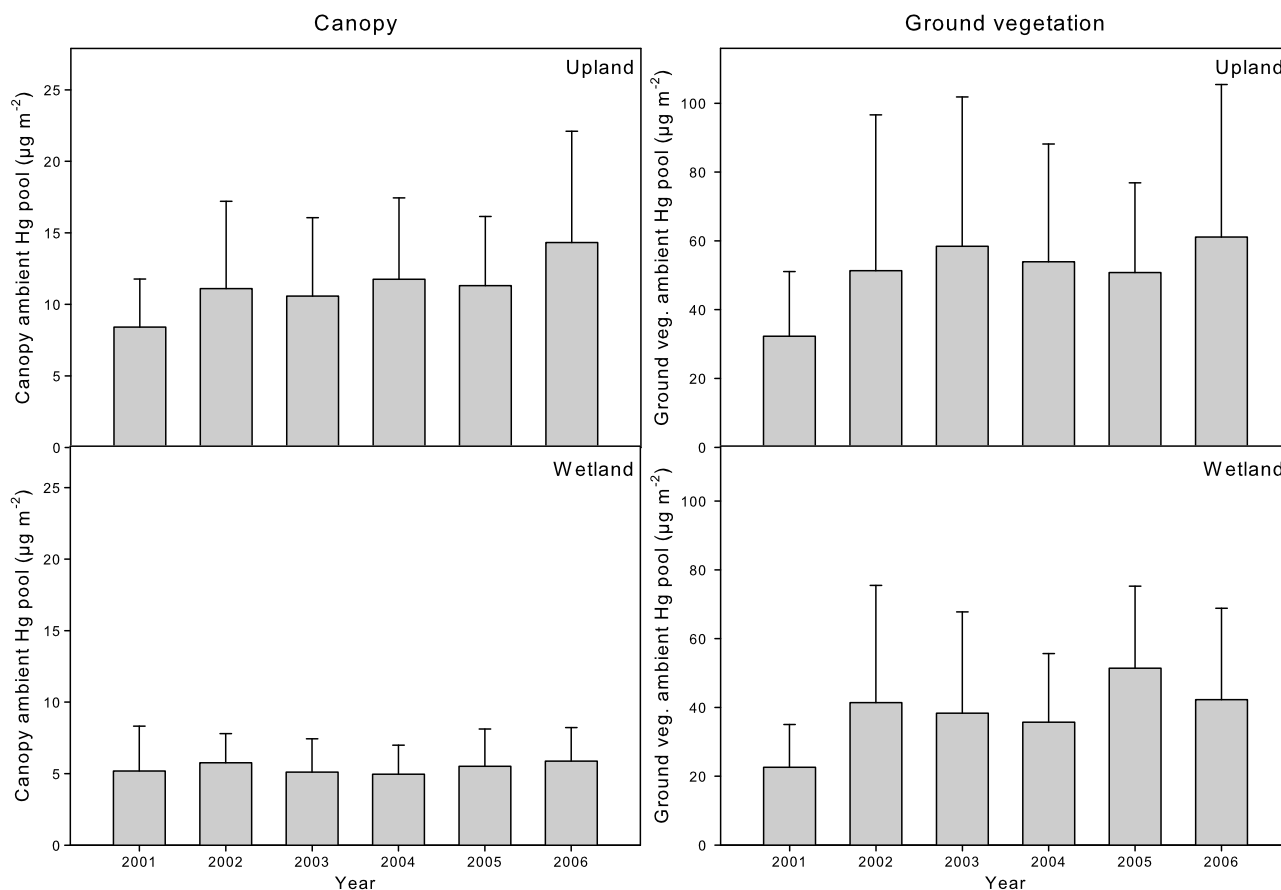


**Figure 5.** Modeled pools of (top) upland and (bottom) wetland ambient Hg in (left) canopy vegetation and (right) ground vegetation within the Lake 658 watershed over the course of METAALICUS experimental Hg loading.

jack pine ( $5.1 \pm 1.7 \mu\text{g m}^{-2}$ , 1.6 times open), deciduous forest ( $4.5 \pm 0.05 \mu\text{g m}^{-2}$ , 1.5 times open) and wetland ( $8.3 \pm 2.6 \mu\text{g m}^{-2}$ , 2.7 times open deposition) forest canopies were always higher than in the open. Average annual litterfall Hg deposition under the mature spruce/fir ( $13.0 \pm 6.9 \mu\text{g m}^{-2}$ ), wetland ( $8.0 \pm 3.0 \mu\text{g m}^{-2}$ ), deciduous ( $7.7 \pm 1.4 \mu\text{g m}^{-2}$ ), and jack pine canopies ( $7.8 \pm 2.1 \mu\text{g m}^{-2}$ ) were within the range of recent values for litterfall deposition of Hg at other North America sites ( $10\text{--}16 \mu\text{g m}^{-2}$ ) [Rea et al., 2002; Sheehan et al., 2006; Demers et al., 2007; Bushey et al., 2008] (Figure S4). Much higher loadings of Hg beneath forest canopies (i.e., throughfall plus litterfall inputs) than in open area deposition have been reported at numerous other sites globally [Munthe et al., 2004, and references therein] and demonstrate the importance of land cover and especially terrestrial vegetation in elevating Hg deposition to the landscape.

### 3.1.2. Ground Vegetation

[30] Average ( $\pm$ S.D.) ambient Hg concentrations of upland and wetland ground vegetation in this study were  $86 \pm 34$  and  $47 \pm 12 \text{ ng g}^{-1}$ . These concentrations are comparable to previously published values for lichen ( $17.2\text{--}66.9 \text{ ng g}^{-1}$ ) [Rasmussen, 1994; Moore et al., 1995] and ground-growing mosses ( $35.1\text{--}286.9 \text{ ng g}^{-1}$ ) [Moore et al., 1995] for the same area (Ontario, Precambrian shield). The upland ground vegetation ambient Hg pool ranged

between a low in 2001 of  $32.3 \pm 18.8 \mu\text{g m}^{-2}$  and a high in 2006 of  $61.1 \pm 44.3 \mu\text{g m}^{-2}$ , and as for the canopy, loads of ambient Hg in different years were not different within error. The wetland ground vegetation ambient Hg pool ranged from  $22.6 \pm 12.5 \mu\text{g m}^{-2}$  in 2001 to  $51.3 \pm 23.8 \mu\text{g m}^{-2}$  in 2005. The average areal mass of ambient Hg in Lake 658 watershed upland ground vegetation was lower but comparable to that observed at the nearby upland microcatchment (UIF) over the same time frame ( $104 \pm 49 \mu\text{g m}^{-2}$ ) [Graydon et al., 2009].

## 3.2. Spike Hg Pools and Fluxes

### 3.2.1. Canopy

[31] The forest canopy is the first watershed compartment that the spike contacted as it was being deposited, and as such, it had the potential to intercept and retain a portion of the spike over some time frame. The canopy pool of spike Hg due solely to annual spray events (gray bars; Figure 6) showed an extremely large range due to differences in annual experimental loading. For example, the wetland canopy spike pool due to the 2002 and 2005 spray events were both  $0 \mu\text{g m}^{-2}$  because only the un-treed wetland shoreline was sprayed in those years. Similarly, the lowest pool of upland spike due to an annual spray also occurred in 2005 ( $0.2 \pm 0.1 \mu\text{g m}^{-2}$ ), when only the upland shoreline was sprayed, which contains few trees. The canopy spike pool due to the

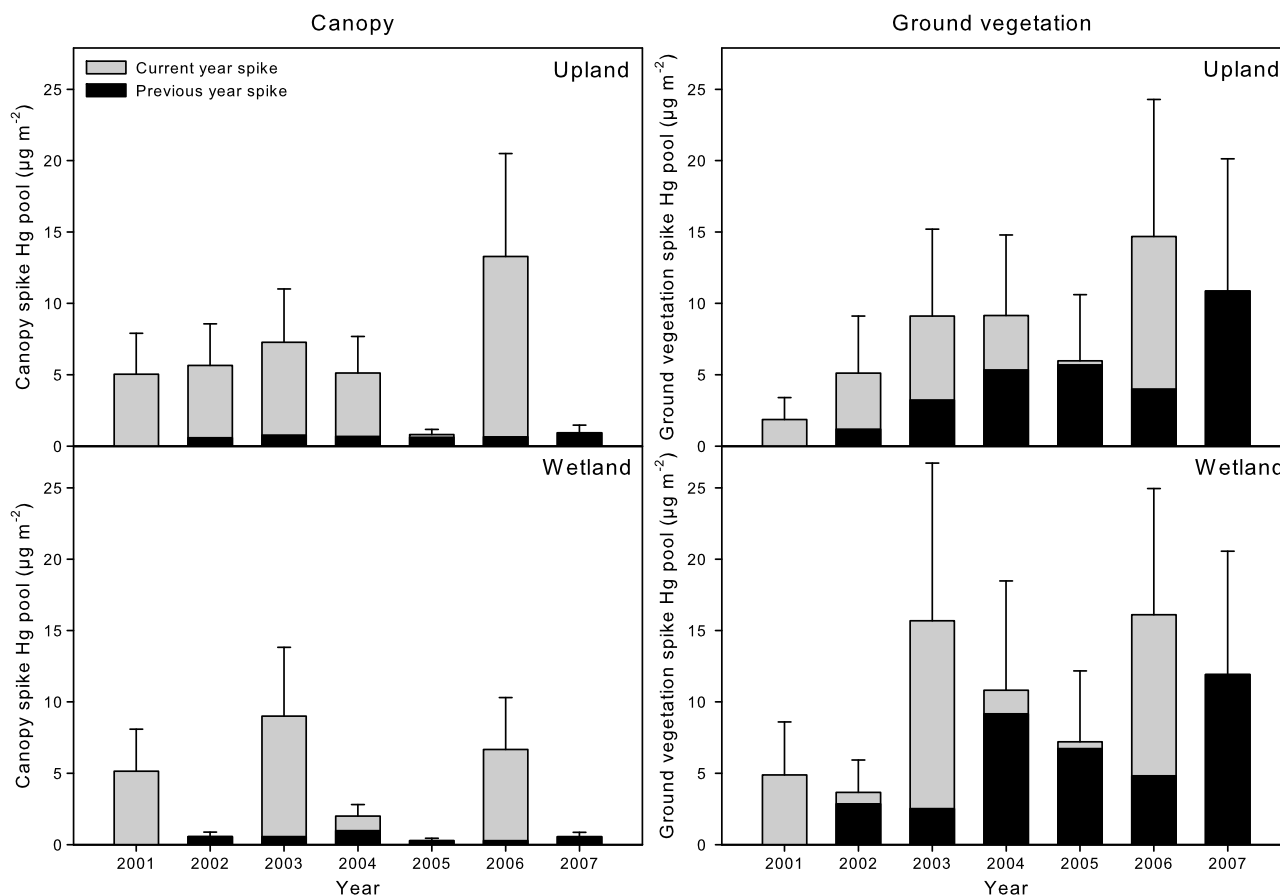


**Figure 6.** Modeled pools of (top) upland and (bottom) wetland spike Hg in (left) canopy vegetation and (right) ground vegetation within the Lake 658 watershed. Gray bars indicate spike Hg mass due to the current year application whereas black bar indicates spike Hg remaining within the canopy from previous applications.

annual spray also exhibited very high levels in some years when most of the watershed received a double-dose of spike because it could not be sprayed the previous year (e.g., 2003 [ $6.6 \pm 3.7 \mu\text{g m}^{-2}$ ] and 2006 [ $5.0 \pm 2.9 \mu\text{g m}^{-2}$ ] for the wetland and 2006 [ $12.6 \pm 7.2 \mu\text{g m}^{-2}$ ] for the upland, Figure 6).

[32] The proportion of the total initial canopy spike pool present just after the spray that still remained immediately prior to the next spray ranged from 2.4–8.7% for deciduous canopies and from 8.3–22% for coniferous canopies. The proportion retained depended on the length of time between spikes, with longer intervals resulting in a lower proportion of spike being present when the next spike was applied (Figure 3). When half-lives of spike on conifer and deciduous foliage were compared for years when the canopy was sampled with sufficient regularity to generate spike concentration decline curves (2001–2004), those of coniferous trees were consistently longer (average  $180 \pm 40$  days), than those of deciduous trees (average  $110 \pm 30$  days), though not statistically significantly so (paired t-test,  $p = 0.068$ ; Table 2). The consistent difference between proportions of spike retained over time (i.e., different half-lives) for deciduous versus coniferous areas is due to the annual senescence and drop of all deciduous foliage in the fall (carryover of spike within deciduous canopies into the next spring was

most likely on branch bark). In contrast, coniferous foliage is longer lived and needles drop asynchronously after life spans of several years in some species. Average annual litterfall spike fluxes ranged from  $0.12 \pm 0.09 \mu\text{g m}^{-2}$  (wetland, 2002) to  $2.3 \pm 1.8 \mu\text{g m}^{-2}$  (upland, 2006) and, like the canopy spike pools themselves, were dependent on the amount of spike applied in different years (Figure S4). Using litterfall spike fluxes at individual sites, the proportion of the

**Table 2.** Decline Curve Rate Constant ( $k$ ) and Half-Life of Spike Hg in Coniferous and Deciduous Canopy Foliage in the Lake 658 Watershed During the First Four Years of the METAALICUS Experiment

Year <sup>b</sup>	$k^a$ (standard error)		Half-Life ( $t_{1/2}$ ) (days)	
	Conifer	Deciduous	Conifer	Deciduous
2001	-0.0029 (0.0011)	-0.0077 (0.0014)	236	90
2002	-0.0045 (0.0007)	-0.0051 (0.0016)	154	136
2003	-0.0049 (0.0004)	-0.0093 (0.0013)	142	75
2004	-0.0035 (0.0004)	-0.0054 (0.0016)	199	129

<sup>a</sup>Decline curve rate constant ( $k$ ) is calculated as the slope of  $\text{Ln } \% \text{ of initial spike concentration}$ .

<sup>b</sup>The years 2001–2004 represent years where the canopy was sampled enough times (i.e.,  $>2$  times post-spray) to generate spike concentration decline curves.

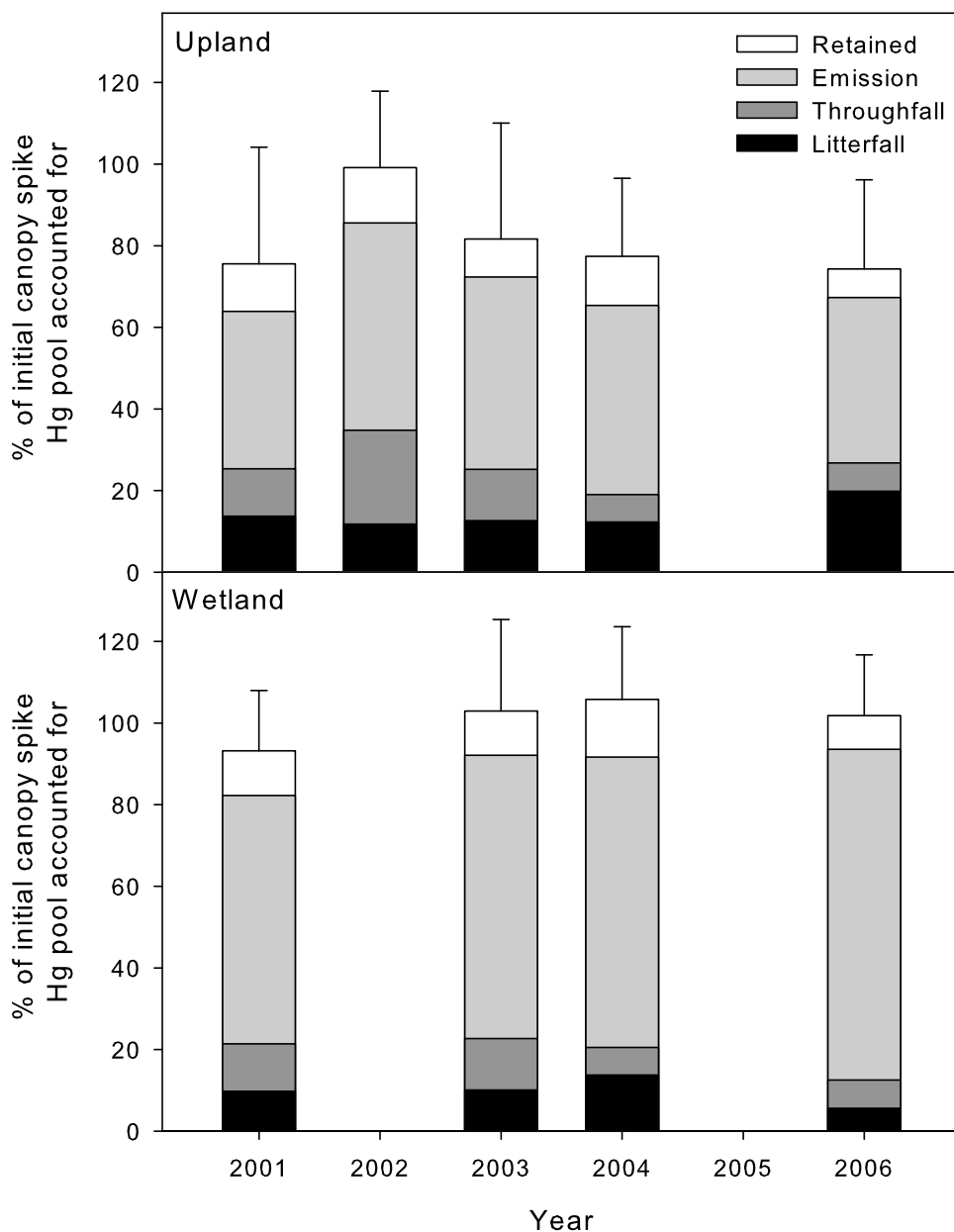


**Figure 7.** Proportion of the total (top) upland and (bottom) wetland canopy spike Hg pools initially present in Lake 658 forest canopies after annual spray events accounted for by the re-emission, throughfall and litterfall fluxes and retention until the following year.

initial total post-spike pool (including new and old spike) accounted for by the litterfall flux was calculated and ranged between 12–20% in the upland and 6–14% in the wetland (Figure 7).

[33] Photoreduction and emission back to the atmosphere of newly deposited spike as Hg(0) is another mechanism by which Hg that is initially retained on foliage can leave the canopy. After the 2003 aerial spike Hg(II) applications to the METAALICUS watershed, the highest initial spike Hg(0) re-emission rates were observed from trees with the highest initial spike Hg concentrations (e.g.,  $26.5 \text{ ng m}^{-2} \text{ hr}^{-1}$  and  $23.8 \text{ ng g}^{-1}$  respectively for upland jack pine; Figure S5). Spike Hg(0) re-emission rates declined rapidly over the next few days and leveled off to near detection limits by the

end of the season. Foliar concentrations of spike Hg on all trees showed a consistent rapid decline after spray application. For example, by 100 days post-spray, average foliar concentrations of spike Hg of these four trees were only 35% (range of 16–55%) of their initial concentrations. Most of the decrease in foliar spike Hg concentration occurred within approximately the first 15 days post-spray and after this initial loss period, concentrations decreased much more slowly or remained constant. Initial foliage spike concentration was positively related to the total  $\mu\text{g m}^{-2}$  of spike evaded from the studied sites ( $y = 0.349x$ ,  $R^2 = 0.90$ ,  $p = 0.05$ ) and emission of spike as Hg(0) (measured using flux chambers) accounted for  $45 \pm 5\%$  and  $71 \pm 8\%$  of the total post-spray canopy spike pool in the upland and wetland,

**Table 3.** Areal Masses of Spike Hg in Canopy, Ground and Total Vegetation Pools Due to Annual Spray Events and the Proportion of Spike Applied Annually to the Upland and Wetland Accounted for in These Pools

Spike	Year	Spike Hg Applied Within Upland or Wetland ( $\mu\text{g m}^{-2}$ )	Canopy Spike Hg Pool ( $\mu\text{g m}^{-2}$ ) (% of applied)	Ground Vegetation Spike Hg Pool ( $\mu\text{g m}^{-2}$ ) (% of applied)	Total Vegetation Spike Hg Pool ( $\mu\text{g m}^{-2}$ ) (% of applied)
Upland	2001	13.3	5.0 (38)	1.9 (14)	6.9 (52)
	2002	20.7	5.1 (24)	3.9 (19)	9.0 (43)
	2003	22.7	6.5 (29)	5.9 (26)	12.4 (55)
	2004	15.1	4.4 (29)	3.8 (25)	8.2 (54)
	2005	1.1	0.2 (17)	0.3 (25)	0.5 (42)
	2006	38.3	12.6 (33)	10.7 (28)	23.3 (61)
Wetland	2001	18.6	3.2 (17)	4.1 (22)	7.3 (39)
	2002	2.7	0.0 (0)	0.8 (29)	0.8 (29)
	2003	41.3	6.5 (16)	11.3 (27)	17.9 (43)
	2004	5.1	0.8 (15)	1.4 (28)	2.2 (43)
	2005	1.2	0.0 (0)	0.0 (39)	0.5 (39)
	2006	38.0	5.0 (13)	9.8 (26)	14.8 (39)

respectively (Figure 7). As such, photoreduction and emission to the atmosphere as Hg(0) likely represents the single largest mechanism of loss of newly deposited spike Hg that is initially intercepted by the canopy. It seems likely that this could be equally true for newly deposited ambient Hg from rain. A similar decline in foliar ambient Hg concentration over time would not be expected however, because of constant re-loading of new Hg from rain events and other major and complicating inputs of ambient Hg to leaves including dry deposition of RGM and PHg to foliar surfaces and especially stomatal uptake of atmospheric Hg(0).

[34] Hg can also be transported from the canopy to the forest floor in precipitation that passes through the forest canopy. Spike that passed through the canopy during the aerial spike applications themselves should be accounted for in the estimates of the initial ground vegetation (this study, see below) and soil spike pools, and the runoff spike flux [Harris *et al.*, 2007]. Throughfall spike concentrations and fluxes were highest in the first samples after collectors were re-deployed following aerial sprays (Figure S6) and levels generally declined until sampling ended in mid-October. Spike concentrations were generally above detection even in years when the watershed was not sprayed, though sites that did not receive a direct hit during the annual aerial spray had samples where spike was not detected (e.g., U19 in 2006). Similar to litterfall and re-emission of spike, throughfall spike fluxes were extremely variable between sites due to the heterogeneity in the aerial spike applications (Figure S6). Open water season throughfall spike Hg flux ranged from 0 to  $3.3 \mu\text{g m}^{-2}$  in the upland and from 0.2 to  $1.5 \mu\text{g m}^{-2}$  in the wetland. The flux of spike in throughfall during winter averaged  $0.005 \pm 0.008 \mu\text{g m}^{-2}$  across all sites and never exceeded  $0.02 \mu\text{g m}^{-2}$ . The throughfall spike flux accounted for  $12 \pm 7\%$  and  $10 \pm 3\%$  of the initial canopy upland and wetland spike pools, respectively (Figure 7). These calculated throughfall fluxes likely represent underestimates of the true total as winter loadings in throughfall were not always available for inclusion and estimates do not include periods of time between shut down of wet deposition collectors (mid-October) and the end of rainfall (typically late October).

[35] Another possible contributing factor to the decline in the concentration of canopy vegetation, that was not accounted for in the modeling of the canopy spike Hg pools, is growth dilution. However, the drop in foliar spike content

is so rapid after application that it seems very unlikely that it is driven to a significant extent by growth dilution. For example, over the first 10 days after the 2003 spray, a 54% drop in spike concentration of foliage was observed whereas the weight of new foliage only increased 7% over the same time [Graydon *et al.*, 2006]. Additionally, the pattern of rapid initial spike concentration decline (and by extension canopy spike half-life) is similar in all years of the experiment, even in 2004 when the canopy was not sprayed until August. In late summer, leaves are at their maximum size and no growth dilution is occurring.

### 3.2.2. Ground Vegetation

[36] Pools of new spike (due to the annual sprays; gray bars in Figure 6) in L658 ground vegetation followed a similar general pattern (in terms of their annual variability) as those in the forest canopy, again because of irregularity in spike application. The average proportion of the total post-spray pool that was retained before the next spray was  $65 \pm 5\%$  over the course of the experiment for both upland and wetland areas alike, much larger than seen in the forest canopy. Average  $t_{1/2}$  of spike on L658 ground vegetation was 890 days (range of 740–1120 days or  $\sim 2$ –3 years based on the standard error of  $k$ ) which was much longer compared to the average  $t_{1/2}$  of spike on coniferous ( $180 \pm 40$  days) and deciduous canopy ( $110 \pm 30$  days) vegetation. Increased light and turbulence within the forest canopy compared to near the forest floor could have driven removal of the spike from the canopy by gaseous emission to a greater extent than from the ground vegetation. The average  $t_{1/2}$  of spike on L658 ground vegetation was also larger (but within error) than the average  $t_{1/2}$  of the 4 spikes applied to ground vegetation at a nearby microcatchment pilot study site called U1F ( $704 \pm 52$  days) [Graydon *et al.*, 2009]. Ground vegetation beneath the L658 canopy is more sheltered and likely received less light than the ground vegetation at U1F, which is located within a more open and exposed rocky upland area. Additionally, U1F spikes were applied directly to the ground vegetation by hand spray, not to the overstory canopy [Hintelmann *et al.*, 2002], a method resulting in no further inputs of spike to U1F ground vegetation after the hand applications were completed. In contrast, litterfall and throughfall represent additional, ongoing sources of upland and wetland spike to L658 ground vegetation after the spike was applied from the plane. Via these two fluxes, some of the

spike initially held in the canopy migrated from that compartment to the forest floor where it accumulated (at least over the timeframe of this study). Ground vegetation pools may also have had higher LAI and/or lower foliage turnover rates, both of which would lead to more efficient scavenging and retention of spike by ground than by canopy vegetation over time. For these reasons, the old or “leftover pre-spray” component of the total ground vegetation spike pool following a spray (black bars in Figure 6), ramped up over the course of the experiment, in sharp contrast to the behavior of the corresponding fraction within the canopy spike pool, which diminished to low levels before the watershed was sprayed once again. Unfortunately it is not possible to comment here on the proportions of the total post-spray ground vegetation spike pool that was evaded or deposited in litterfall or throughfall as was done for the forest canopy.

[37] While a complete mass balance of the spike applied to upland and wetland areas is not possible here, data are being prepared by other research groups including additional pools (soil and peat) and fluxes (emission from ground vegetation, runoff) that are necessary to complete these mass balances. Overall, the average proportion of newly applied spike from the plane accounted for in terrestrial vegetation (canopy plus ground vegetation pools) immediately after spraying was  $53 \pm 6\%$  in the upland and  $41 \pm 2\%$  in the wetland (averages are for years when spike was applied to a greater area than just the shoreline; Table 3). The different retention within upland versus wetland vegetation was primarily a result of difference in forest canopy retention ( $31 \pm 5\%$  and  $15 \pm 2\%$ , respectively), rather than differences in retention in ground vegetation (upland  $22 \pm 6\%$  and wetland  $26 \pm 3\%$ ), because of the more open canopy and lower average LAI of the wetland (1.2) compared to that of the upland (1.7).

[38] Results from this study suggest that retention of newly wet-deposited Hg on canopy and especially on ground vegetation results in delays in the further downward translocation of significant amounts of new Hg into the organic soil layer. Consequently this Hg cannot immediately run off into adjacent lakes, supporting previous observations that runoff Hg includes mostly older Hg deposited some time ago. In an earlier experiment where an enriched isotopic Hg spike was applied to soil plots, 30% of the spike was retained in soils over the following 16 months [Munthe et al., 2001]. Similarly, initial mobility of the spike applied to ground vegetation of the UIF microcatchment (ELA) declined rapidly and after a few months,  $< 1\%$  was exported in runoff, 8% had evaded to the atmosphere and 66% was still bound to ground vegetation. The spike quickly equilibrated with ambient Hg pools in vegetation and soils, rendering it basically immobile over the short-term [Hintelmann et al., 2002]. Hg bound to vegetation may only be delivered into the soil pool during senescence and litterfall and even longer delays can be expected as litterfall must likely decompose to some degree to release bound Hg to underlying soils. It has also recently been demonstrated that newly deposited litterfall absorbs Hg from underlying soils and this internal recycling further increases the residence time of Hg within the forest floor [Hall and St. Louis, 2004; Demers et al., 2007].

[39] **Acknowledgments.** Contribution 36 of the Mercury Experiment to Assess Atmospheric Loading in Canada and the United States (METAALICUS). We thank summer students Shawn Harriman, Jasmin Finch, Joanna Januszkiewicz, Eric Ong, Sarah Downey, and Linnea Mowat.

We also greatly appreciate field and laboratory help from Justin Shead, Brian Dimock, Sara Berkel, Z McLatcher, Po Yee Chan, April Zembal, and Caroline Lee. Tarmo Rimmel provided hemispherical photographs of the canopy for LAI measurements. This project was funded through grants from the Natural Sciences and Engineering Research Council of Canada (NSERC), Collaborative Mercury Research Network (COMERN), Canadian Circumpolar Institute, Electric Power Research Institute (EPRI), the Department of Fisheries and Oceans Canada, the Alberta Heritage Fund, and the University of Alberta. S.E.L. was supported in part by EPA STAR grant RD833378010.

## References

- Asmuth, H. (2005), Vertical decomposition of forest structure using LiDAR remote sensing, MS thesis, Dep. of Geogr., Univ. of Toronto, Mississauga, Mississauga, Ont., Canada.
- Barghigiani, C., T. Ristori, and R. Bauleo (1991), Pinus as an atmospheric Hg biomonitor, *Environ. Technol.*, *12*(12), 1175–1181, doi:10.1080/09593339109385118.
- Bombosch, S. (1983), Mercury-accumulation in game, in *Effects of Accumulation of Air Pollutants in Forest Ecosystems*, edited by B. Ulrich and J. Pankrath, pp. 271–281, D. Reidel, Hingham, Mass.
- Bushey, J. T., A. G. Nallana, M. R. Montesdeoca, and C. T. Driscoll (2008), Mercury dynamics of a northern hardwood canopy, *Atmos. Environ.*, *42*, 6905–6914, doi:10.1016/j.atmosenv.2008.05.043.
- Converse, A. D., A. L. Riscassi, and T. M. Scanlon (2010), Seasonal variability in gaseous mercury fluxes measured in a high-elevation meadow, *Atmos. Environ.*, *44*, 2176–2185, doi:10.1016/j.atmosenv.2010.03.024.
- Demers, J. D., C. T. Driscoll, T. J. Fahey, and J. B. Yavitt (2007), Mercury cycling in litter and soils in different forest types in the Adirondack region, New York, USA, *Ecol. Appl.*, *17*, 1341–1351, doi:10.1890/06-1697.1.
- Eckley, C. S., and H. Hintelmann (2006), Determination of mercury methylation potentials in the water column of lakes across Canada, *Sci. Total Environ.*, *368*(1), 111–125, doi:10.1016/j.scitotenv.2005.09.042.
- Fleck, J. A., D. F. Grigal, and E. A. Nater (1999), Mercury uptake by trees: An observational experiment, *Water Air Soil Pollut.*, *115*, 513–523, doi:10.1023/A:1005194608598.
- Gilmour, C. C., E. A. Henry, and R. Mitchell (1992), Sulfate stimulation of mercury methylation in fresh-water sediments, *Environ. Sci. Technol.*, *26*(11), 2281–2287, doi:10.1021/es00035a029.
- Gower, S. T., J. G. Vogel, J. M. Norman, C. J. Kucharik, S. J. Steele, and T. K. Stow (1997), Carbon distribution and aboveground net primary production in aspen, jack pine, and black spruce stands in Saskatchewan and Manitoba, Canada, *J. Geophys. Res.*, *102*(D24), 29,029–29,041, doi:10.1029/97JD02317.
- Graydon, J. A., V. L. St. Louis, S. E. Lindberg, H. Hintelmann, and D. P. Krabbenhoft (2006), Investigation of mercury exchange between forest canopy vegetation and the atmosphere using a new dynamic chamber, *Environ. Sci. Technol.*, *40*(15), 4680–4688, doi:10.1021/es0604616.
- Graydon, J. A., V. L. St. Louis, H. Hintelmann, S. E. Lindberg, K. A. Sandilands, J. W. M. Rudd, C. A. Kelly, B. D. Hall, and L. D. Mowat (2008), Long-term wet and dry deposition of total and methyl mercury in the remote boreal ecoregion of Canada, *Environ. Sci. Technol.*, *42*(22), 8345–8351, doi:10.1021/es801056j.
- Graydon, J. A., V. L. St. Louis, H. Hintelmann, S. E. Lindberg, J. W. M. Rudd, C. A. Kelly, K. A. Sandilands, M. T. Tate, D. P. Krabbenhoft, and I. Lehnher (2009), Investigation of uptake and retention of atmospheric Hg(II) by boreal forest plants using stable Hg isotopes, *Environ. Sci. Technol.*, *43*(13), 4960–4966, doi:10.1021/es900357s.
- Grigal, D. F., R. K. Kolka, J. A. Fleck, and E. A. Nater (2000), Mercury budget of an upland-peatland watershed, *Biogeochemistry*, *50*, 95–109, doi:10.1023/A:1006322705566.
- Hall, B. D., and V. L. St. Louis (2004), Methylmercury and total mercury in plant litter decomposing in upland forests and flooded landscapes, *Environ. Sci. Technol.*, *38*(19), 5010–5021, doi:10.1021/es049800q.
- Harris, R. C., et al. (2007), Whole-ecosystem study shows rapid fish-mercury response to changes in mercury deposition, *Proc. Natl. Acad. Sci. U. S. A.*, *104*(42), 16,586–16,591, doi:10.1073/pnas.0704186104.
- Heyes, A., T. R. Moore, and J. W. M. Rudd (1998), Mercury and methylmercury in decomposing vegetation of a pristine and impounded wetland, *J. Environ. Qual.*, *27*(3), 591–599, doi:10.2134/jeq1998.00472425002700030017x.
- Hightower, J. M., and D. Moore (2003), Mercury levels in high-end consumers of fish, *Environ. Health Perspect.*, *111*, 604–608, doi:10.1289/ehp.5837.
- Hintelmann, H., and R. D. Evans (1997), Application of stable isotopes in environmental trace studies—measurement of monomethylmercury ( $\text{CH}_3\text{Hg}^+$ ) by isotope dilution ICP-MS and detection of species

- transformation, *Fresenius J. Anal. Chem.*, 358, 378–385, doi:10.1007/s002160050433.
- Hintelmann, H., and N. Ogrinc (2003), Determination of stable mercury isotopes by ICP/MS and their application in environmental studies, in *Biogeochemistry of Environmentally Important Trace Elements, ACS Symp. Ser.*, vol. 835, edited by Y. Cai and C. O. Braids, pp. 321–338, Am. Chem. Soc., Washington, D. C.
- Hintelmann, H., R. D. Evans, and J. Y. Villeneuve (1995), Measurement of mercury methylation in sediments by using enriched stable mercury isotopes combined with mercury determination by gas-chromatography inductively coupled plasma-mass spectrometry, *J. Anal. At. Spectrom.*, 10(9), 619–624, doi:10.1039/ja9951000619.
- Hintelmann, H., R. Harris, A. Heyes, J. P. Hurley, C. A. Kelly, D. P. Krabbenhoft, S. E. Lindberg, J. W. M. Rudd, K. J. Scott, and V. L. St. Louis (2002), Reactivity and mobility of new and old mercury deposition in a Boreal forest ecosystem during the first year of the METAALICUS study, *Environ. Sci. Technol.*, 36, 5034–5040, doi:10.1021/es025572t.
- Hultberg, H., J. Munthe, and Å. Iverfeldt (1995), Cycling of methylmercury and mercury-responses in the forest roof catchment to three years of decreased atmospheric deposition, *Water Air Soil Pollut.*, 80, 415–424, doi:10.1007/BF01189691.
- Johansson, K., M. Aastrup, A. Andersson, L. Bringmark, and Å. Iverfeldt (1991), Mercury in Swedish forest soils and waters-assessment of critical load, *Water Air Soil Pollut.*, 56, 267–281, doi:10.1007/BF00342276.
- Kidd, K. A., R. H. Hesslein, R. J. P. Fudge, and K. A. Hallard (1995), The influence of trophic level as measured by  $\delta^{15}\text{N}$  on mercury concentrations in freshwater organisms, *Water Air Soil Pollut.*, 80, 1011–1015, doi:10.1007/BF01189756.
- Leblanc, S. G., J. M. Chen, R. Fernandes, D. W. Deering, and A. Conley (2005), Methodology comparison for canopy structure parameters extraction from digital hemispherical photography in boreal forests, *Agric. For. Meteorol.*, 129, 187–207, doi:10.1016/j.agrformet.2004.09.006.
- Lee, Y. H., K. Bishop, and J. Munthe (2000), Do concepts about catchment cycling of methylmercury and mercury in boreal forest catchments stand the test of time? Six years of atmospheric inputs and runoff export at Svartberget, Northern Sweden, *Sci. Total Environ.*, 260, 11–20, doi:10.1016/S0048-9697(00)00538-6.
- Lindberg, S. E., R. Bullock, R. Ebinghaus, D. Engstrom, X. Feng, W. Fitzgerald, N. Pirrone, E. Prestbo, and C. Seigneur (2007), A synthesis of progress and uncertainties in attributing the sources of mercury in deposition, *Ambio*, 36, 19–33, doi:10.1579/0044-7447(2007)36[19:ASOPAU]2.0.CO;2.
- Moore, T. R., J. L. Bubier, A. Heyes, and R. J. Flett (1995), Methyl and total mercury in boreal wetland plants, Experimental Lakes Area, Northwestern Ontario, *J. Environ. Qual.*, 24(5), 845–850, doi:10.2134/jeq1995.00472425002400050007x.
- Munthe, J., and H. Hultberg (2004), Mercury and methylmercury in runoff from a forested catchment - Concentrations, fluxes, and their response to manipulations, *Water Air Soil Pollut. Focus*, 4, 607–618, doi:10.1023/B:WAFO.0000028381.04393.ed.
- Munthe, J., B. Lyvén, H. Parkman, Y.-H. Lee, Å. Iverfeldt, C. Haraldsson, M. Verta, and P. Porvari (2001), Mobility and methylation of mercury in forest soils: Development of an in-situ isotope tracer technique and initial results, *Water Air Soil Pollut. Focus*, 1, 385–393, doi:10.1023/A:1017574103867.
- Munthe, J., et al. (2004), Input-output of Hg in forested catchments in Europe and North America, *RMZ Mater. Geoenvironment*, 51(2), 1243–1246.
- Munthe, J., R. A. Bodaly, B. A. Branfireun, C. T. Driscoll, C. C. Gilmour, R. Harris, M. Horvat, M. Lucotte, and O. Malm (2007), Recovery of mercury-contaminated fisheries, *Ambio*, 36(1), 33–44, doi:10.1579/0044-7447(2007)36[33:ROMF]2.0.CO;2.
- Rasmussen, P. E. (1994), Current methods of estimating atmospheric mercury fluxes in remote areas, *Environ. Sci. Technol.*, 28(13), 2233–2241, doi:10.1021/es00062a006.
- Rasmussen, P. E. (1995), Temporal variation of mercury in vegetation, *Water Air Soil Pollut.*, 80(1–4), 1039–1042, doi:10.1007/BF01189762.
- Rasmussen, P. E., G. Mierle, and J. O. Nriagu (1991), The analysis of vegetation for total mercury, *Water Air Soil Pollut.*, 56, 379–390, doi:10.1007/BF00342285.
- Rea, A. W., G. J. Keeler, and T. Scherbatskoy (1996), The deposition of mercury in throughfall and litterfall in the lake Champlain watershed: A short-term study, *Atmos. Environ.*, 30(19), 3257–3263, doi:10.1016/1352-2310(96)00087-8.
- Rea, A. W., S. E. Lindberg, T. Scherbatskoy, and G. J. Keeler, (2002), Mercury accumulation in foliage over time in two northern mixed-hardwood forests, *Water Air Soil Pollut.*, 133, 49–67, doi:10.1023/A:1012919731598.
- Sandilands, K. A., J. W. M. Rudd, C. A. Kelly, H. Hintelmann, C. C. Gilmour, and M. T. Tate (2005), Application of enriched stable mercury isotopes to the Lake 658 watershed for the METAALICUS project, at the Experimental Lakes Area, northwestern Ontario, Canada, *Can. Tech. Rep. Fish. Aquat. Sci.*, 2597, 48 pp.
- Sandilands, K. A., C. A. Kelly, J. W. M. Rudd, M. T. Tate, H. Hintelmann, B. Dimock, and R. Harris (2008), Application of enriched stable mercury isotopes to the Lake 658 watershed for the METAALICUS project, at the Experimental Lakes Area, northwestern Ontario, Canada, 2001–2007. *Can. Tech. Rep. Fish. Aquat. Sci.*, 2813, 38 pp.
- Sheehan, K. D., I. J. Fernandez, J. S. Kahl, and A. Amirbahman (2006), Litterfall mercury in two forested watersheds at Acadia National Park, Maine, USA, *Water Air Soil Pollut.*, 170, 249–265, doi:10.1007/s11270-006-3034-y.
- St. Louis, V. L., J. W. M. Rudd, C. A. Kelly, K. G. Beaty, N. S. Bloom, and R. J. Flett (1994), Importance of wetlands as sources of methyl mercury to boreal forest ecosystems, *Can. J. Fish. Aquat. Sci.*, 51, 1065–1076, doi:10.1139/f94-106.
- St. Louis, V. L., J. W. M. Rudd, C. A. Kelly, B. D. Hall, K. R. Roloffus, K. J. Scott, S. E. Lindberg, and W. Dong (2001), Importance of the forest canopy to fluxes of methyl mercury and total mercury to boreal ecosystems, *Environ. Sci. Technol.*, 35(15), 3089–3098, doi:10.1021/es001924p.
- Stokstad, E. (2008), Canada's experimental lakes, *Science*, 322, 1316–1319, doi:10.1126/science.322.5906.1316.
- Swain, E. B., D. R. Engstrom, M. E. Brigham, T. A. Henning, and P. L. Brezonik (1992), Increasing rates of atmospheric mercury deposition in midcontinental North America, *Science*, 257, 784–787, doi:10.1126/science.257.5071.784.
- Wytenbach, A., and L. Tobler (1988), The seasonal variation of 20 elements in 1st and 2nd year needles of Norway spruce, *Picea abies* (L.) Karst, *Trees*, 2, 52–64, doi:10.1007/BF01196345.

H. Asmath, Department of Geography, University of Toronto, Mississauga, 3359 Mississauga Rd. N., South Bldg., Mississauga, ON L5L 1C6, Canada.  
C. A. Emmerton, J. A. Graydon, and V. L. St. Louis, Department of Biological Sciences, University of Alberta, Edmonton, AB T6G 2E9, Canada. (jgraydon@ualberta.ca)

R. Harris, Reed Harris Environmental Ltd., 180 Forestwood Dr., Oakville, ON L6J 4E6, Canada.

C. A. Kelly and J. W. M. Rudd, R&K Research Inc., 675 Mt. Belcher Heights, Salt Spring Island, BC V8K 2J3, Canada.

D. P. Krabbenhoft and M. T. Tate, Water Resources Division, U.S. Geological Survey, 8505 Research Way, Middleton, WI 53562, USA.

S. E. Lindberg, Oak Ridge National Laboratory, PO Box 2008, Oak Ridge, TN 37831-6083, USA.

M. Richardson, Department of Geography and Environmental Studies, Carleton University, 1125 Colonel By Drive, Ottawa, ON K1S 5B6, Canada.

K. A. Sandilands, Freshwater Institute, Fisheries and Oceans Canada, 501 University Dr., Winnipeg, MB R3T 2N6, Canada.